Partial depolymerization of tamarind seed xyloglucan and its functionality toward enhancing the solubility of curcumin

Weeranuch Lang[1,*], Takayoshi Tagami[1], Hye-Jin Kang[1], Masayuki Okuyama[1], Nobuo Sakairi[2], Atsuo Kimura[1,*]

[1]Laboratory of Molecular Enzymology, Research Faculty of Agriculture, Hokkaido University, Sapporo 060-8589, Japan

[2]Division of Environmental Materials Science, Faculty of Environmental Earth Science, Hokkaido University, Sapporo 060-0810, Japan

[*]Corresponding author: tel/fax, +81 11 706 2808; e-mail addresses, kimura@abs.agr.hokudai.ac.jp (A. Kimura) and weranuch@abs.agr.hokudai.ac.jp (W. Lang).

E-mail addresses: weranuch@abs.agr.hokudai.ac.jp, weranuch24@hotmail.com (W. Lang), tagami@abs.agr.hokudai.ac.jp (T. Tagami), hyejin@abs.agr.hokudai.ac.jp (H. J. Kang), okuyama@abs.agr.hokudai.ac.jp (M. Okuyama), nsaka@ees.hokudai.ac.jp (N. Sakairi), kimura@abs.agr.hokudai.ac.jp (A. Kimura).

Abstract

Polysaccharides of tamarind seed, a byproduct of the tamarind pulp industry, displayed a potential solubility improvement of lipophilic bioactive molecules but their textural characteristics hinder the dietary formulation. In contrast, the commonly available xyloglucan oligosaccharides (XOSs) with degrees of polymerization (DPs) of 7, 8, and 9 were too short to maintain their ability. The binding capacity of the between sizes is unknown due to a lack of appropriate preparation. We prepared xyloglucan megalosaccharides (XMSs) by partial depolymerization, where term megalosaccharide (MS) defines the middle chain-length saccharide between DPs 10–100. Digestion with fungal cellulase enabled reproducible active XMSs. Further identification of pure XMS segments indicated that XMS-B has an average DP of 17.2 ($Gal_3Glc_8Xyl_6$) with a branched dimer of XOS 8 and 9 and was free of side-chain arabinose, the residue influencing high viscosity. Curcumin, a bioactive pigment, has poor bioavailability because of its water insolubility. XMSs with average DPs of 15.4–24.3 have similarly sufficient capacities to solubilize curcumin. The solubility of curcumin was improved 180-fold by the addition of 50%, w/v, XMSs, which yielded a clear yellow liquid. Our findings indicated that XMSs were a promising added-value agent in foods and pharmaceuticals for the oral intake of curcumin.

Keywords: acid hydrolysis, cellulase, hydrophobic interaction, tamarind gum, *Trichoderma viride*, xyloglucan megalosaccharide

Abbreviations

AN, *Aspergillus niger* cellulase; DP, degree of polymerization; HCl, hydrochloric acid; HPAEC-PAD, high-performance anion exchange chromatography with pulsed amperometric detection; K_s, equilibrium constant; K_c, association constant; MW, molecular weight; TV, *Trichoderma viride* cellulase; XMS, xyloglucan megalosaccharide; XOS, xyloglucan oligosaccharide; YC, *Trichoderma viride* cellulase.

1. Introduction

Some polysaccharides display a strong affinity for hydrophobic binding to nonpolar molecules based on their fine structure of monosaccharide compositions, linkages, and degree of polymerization (DP). Their intrinsic characteristics, including viscosity and swelling degree, may slightly promote this binding interaction but highly influence the limitation of the dietary formulation in health sciences to be mainly a heterogeneous form, e.g., tablet, capsule, powder, etc. (Sapkal, Narkhede, Babhulkar, Mehetre, & Rathi, 2013; Viral, Dhiren, Mane, & Umesh, 2010). Xyloglucan is a major structure of plant hemicellulose found abundant in tamarind (*Tamarindus indica* L.) seed gum, which is a byproduct of the tamarind pulp industry. According to the structural configuration, Janado & Yano (1985) suggested that two aldopentoses, D-xylose and L-arabinose, predominantly possess superior hydrophobicity among other monosaccharides, where D-galactose and D-glucose are highly water-soluble aldohexoses facilitating chain solubility. Since tamarind seed xyloglucan underlies these patterns, we hypothesized that it is a potential source of botanical host molecules to enhance the water solubility of lipophilic ligands if the appropriate size preparation strategy can be established. Tamarind seed xyloglucan is a structurally highly branched heteropolysaccharide with a molecular weight (MW) varying from 650,000 to 2,500,000, and the monomers of glucose, xylose, galactose, and arabinose are contained in a molar ratio of 45:34:18:3 (Majee, Avlani, & Biswas, 2016; Walker et al., 2017). The structure of tamarind seed xyloglucan consists fundamentally of a cellulose-like β-(1→4)-linked glucan backbone where on average, 3 out of 4 glucosyl backbone residues have 1→6 linked xylose substituents. The branches can have galactose and arabinose substituents where the galactose substituent dominates the water solubility, as its abstraction (45% by β-galactosidase) can compose a thermally reversible gel at physiological temperature and thus utilize as conveyances for nasal drug delivery (Mahajan, Tyagi, Lohiya, & Nerkar, 2012). A minor amount of arabinose units is present at the side chain with a random arrangement (Niemann, Carpita, & Whistler, 1997), and the function is not reported even though a high degree of arabinose substitution in arabinoxylan from rye grain leads to highly viscous

solutions (Bengtsson, Andersson, Westerlund, & Åman 1992). Tamarind seed xyloglucan is a non-nutrient and is widely applied for thickening, stabilizing, and gelling agents in the food industry. Similarly, xyloglucan oligosaccharides (XOSs) are also obtained from tamarind seed xyloglucan by exhaustive digestion with fungal endo-(1→4)-β-D-glucanases (Satoh, Tateishi, & Sugiyama, 2013). They are classified into three different structures for the repeating units of tamarind seed xyloglucan: heptasaccharide (Glc_4Xyl_3, XOS 7, octasaccharide (Glc_4Xyl_3Gal, XOS 8), and nonasaccharide ($Glc_4Xyl_3Gal_2$, XOS 9). They are likely the active ingredients associated with flower opening in carnation and inhibitory effects on the absorption of D-glucose in the intestine (Satoh et al., 2013; Sone & Sato, 1994). From the aforementioned, tamarind seed xyloglucan and XOSs have various industrial and pharmaceutical applications. However, the potency of their middle size denoting saccharides with DPs of 10–100, a term "megalosaccharide" (MS) originally proposed by French and his colleagues (Thoma, Wright, & French, 1959), has not been intensively used to date since there were no appropriate preparations of the sample sizes. Although tamarind seed xyloglucan is edible, the consumption is not practically in households due to its poor textural characteristics of the highly viscous. XMS is probably more soluble and less viscous in water but its preparation and functionality remain unclear.

Curcumin is a yellow lipid-soluble phenolic pigment present in the spice turmeric (*Curcuma longa*). It has various therapeutic potential and biological activities, such as anti-inflammatory and antioxidant activities, as denoted by over 6,000 citations (Prasad, Tyagi, & Aggarwal, 2014). However, practical water insolubility (0.54 μM or 0.2 μg/mL), which is eventually responsible for poor stability and poor bioavailability, has been highlighted as a major issue. Various types of curcumin forms have been designed to improve bioavailability, including chemical modification, nanoparticles, micelles, liposomes, and lipidic nanoparticles possessing an internal cubic phase structure (Yadav et al., 2020; Wu et al., 2020; Victorelli et al., 2022). In addition, some additives, such as resveratrol/lactoglobulin, cyclodextrin, steviol glycoside, and poly-(lactic-*co*-glycolic acid), are considerably attributed to the increased solubility of curcumin (Zhang et al., 2022; Mangolim et al., 2014; Nguyen et al., 2017; Sharma et al., 2021). Here, we proposed a different approach to solubilize curcumin for its potent use. The objective of this study was to establish preparation methods for functional XMSs from tamarind seed polysaccharides and provide a systematic study of the real binding capacity between curcumin and the fine structures of XMSs.

In this study, we first evaluated the solubilizing ability of curcumin by tamarind seed xyloglucan compared with other water-soluble plant and algae polysaccharides, including λ-carrageenan, gum arabic, guar gum, pectin, and amylopectin, to screen the functional polysaccharide source. XMS was then prepared by acid and enzyme digestions of tamarind seed xyloglucan and further fractionated by methanol since they are uncomplicated implements. The

complex formation of XMS and curcumin was verified by a fluorescent approach to provide fundamental knowledge of the real binding.

2. Materials and methods

2.1. Preparation of XMSs and their isolation. Acid and enzyme hydrolyses were carried out as follows: a 1% w/v slurry of tamarind seed xyloglucan (high purity grade, Tokyo Chemical Industry, Tokyo, Japan, 2 g) was prepared in 200 ml of water (for acid) and 50 mM sodium phosphate buffer, pH 6.0 (for the enzyme) and subsequently heated by microwave and vigorously stirred until boiling 2–3 times to have a homogeneous form; and then partially hydrolyzed by hydrochloric acid (HCl) solution or cellulases. The former was performed by the addition of hot HCl (4 M; preheated at 80 °C) to obtain a final concentration of 0.5 M and incubated for 2, 4, and 5 h at 80 °C, followed by neutralization with 4.0 M sodium hydroxide in an ice bath. The latter was performed with *Trichoderma viride* cellulase (TV, Sigma–Aldrich, Tokyo, Japan), *Aspergillus niger* cellulase (AN, Nacalai Tesque, Kyoto, Japan), and *Trichoderma viride* cellulase from Seshin Pharmaceutical, Tokyo, Japan (YC). The reaction mixtures were carried out at 37 °C for 2 h utilizing individual fungal cellulases of 9.5 units, and the samples were autoclaved at 121 °C for 15 min to inactivate the enzyme. Thereafter, 90%, v/v, methanol was integrated while mixing, and the digested samples were placed in ice water for an additional 2 h. The precipitant was isolated by centrifugation at 13,000 ×*g* for 30 min, evaporated, and dried under a vacuum. The enzyme activity determined for the above three commercial cellulases (TV, YC, and AN) was 0.033, 0.027, and 0.012 unit/mg solid, respectively, whereas one unit is the amount of enzyme that liberates 1 μmol of glucose from sodium carboxymethyl cellulose (Sigma, 0.5%, w/v) per minute in 50 mM sodium phosphate buffer pH 6.0 and 37 °C. For the time course study, the samples were withdrawn at different time intervals until 24 h. Next, the reaction mixture containing 15 g of tamarind seed xyloglucan was prepared again with YC, but the incubation time was fixed at 2 h to collect various sizes of MSs. After autoclaving, the sample was centrifuged at 11,300 ×*g* for 30 min and then filtered through a membrane filter (0.2 μm mixed cellulose ester, Advantec, Tokyo, Japan) to remove the insoluble pellet, and the supernatant was desalted by a manually packed ion-exchange column (amberlite MB4, Organo, Tokyo, Japan). The product sizes in the supernatant were isolated into four fractions by sequential methanol precipitation (≤ 60, 60–70, 80–95%, v/v). The shortest fragment containing XOSs was not precipitated. Thus, it was collected after evaporation and dialyzed with a Spectra/Por®6 membrane (Rancho Dominguez, CA, USA) with a MW cutoff of 1 kD against water to discard glucose and oligosaccharides having an average DP less than 6 (referred to as > 95%, v/v).

The yield was expressed as the ratio (%) of the amount of the obtained xyloglucan hydrolyses divided by the amount of the substrate used (15 g). Based on the obtained functional

size results, the methanol concentration was considerably adjusted to 60–75%, v/v to obtain MSs with an average DP of 19. The pellet was dried by lyophilizer (Eyela FDU-1200, Tokyo, Japan) and profiled by Dionex high-performance anion exchange chromatography with pulsed amperometric detection (HPAEC-PAD, CarboPac^{TM} PA1 Column 4 × 250 mm, Dionex Co., Sunnyvale, CA, USA) with an eluent of 16 mM sodium hydroxide for 20 min and further incremented to 200 mM with a sodium acetate gradient of 0–100 mM for 40 min and from 100–250 mM for 20 min. Purification of XOSs and XMS-A and XMS-B from YC digests was performed by preparative HPLC on an Imtakt Unison US-Amino column (20 × 250 mm) with an eluent of 70%, v/v, acetonitrile in water at a flow rate of 4 mL/min for XOS 7–9 and 65%, v/v, at 2 mL/min for XMS-A and XMS-B. Upon evaporation of the solvent, the purities of XOSs, XMS-A, and XMS-B were determined by HPAEC-PAD analysis. These samples were also used as external standards to quantify the concentration of peaks presented in Fig. 3.

2.2. Determination of MW, monosaccharide composition, and DP. The MW of polysaccharides or MSs was individually determined by a gel filtration column of Shodex OHpak SB-806 HQ or SB-803 HQ (8.0 × 300 mm), respectively using the same HPLC apparatus described previously (Lang et al., 2022a). The saccharide samples were dissolved with 5 mg/mL in sodium nitrate solution (0.1 M), centrifuged, and eluted with the same solution at 0.5 mL/min and 40 °C. The signals were detected by a refractive index detector (RI 2031 Plus, JASCO, Tokyo, Japan). The molecular mass markers used were Shodex standard P-82 pullulans (P-800–P-5, Showa Denko K.K., Kanagawa, Japan) and maltoheptaose (G7, Nihon Shokuhin Kako, Tokyo, Japan). The calibration curves were constructed using the retention times and MWs (obtained from the manufacturer instruction) of P-800, P-400, P-200, and P-100 for polysaccharides and P-100, P-50, P-20, P-10, P-5, and G7 for the MS-size samples.

Molecular mass of XMS-A and XMS-B was obtained from ESI mass spectra using Thermo Scientific Exactive spectrometer (Thermo Fisher Scientific, Waltham, MA, USA). All samples were subjected to a nanospray in a positive ion mode, and the recorded mass range was at *m/z* 1,000 to *m/z* 1,500. The major molecular ion on saccharide analysis is usually derived from $[M + H]^+$ or $[M + Na]^+$: one proton or one sodium is added, and then the ion detected is one ($z = 1$). However, in the case of $[M + 2H]^{2+}$ or $[M + 2Na]^{2+}$ for XMSs ($z = 2$), molecular mass by ESI mass spectrometry (positive mode) was calculated as follows: molecular mass = (*m/z* value × z) – 23, where 23 is the mass of the adduct ion of Na^+.

For monosaccharide composition analysis, dried XMS (0.5 mg) was hydrolyzed at 120 °C in 0.1 mL of 2 M trifluoroacetic acid for 2 h in a glass vial. The acid was then removed by nitrogen flushing. The samples were subsequently redissolved in water at the appropriate dilution and analyzed by HPAEC-PAD under isocratic conditions of 16 mM sodium hydroxide, and *myo*-

inositol was utilized as an internal standard [see Fig. S1 containing a typical example of XMS (average DP 63.7 in Table 2)]. The molar concentration of each monosaccharide was determined from peak area using known sugar standard (arabinose, galactose, glucose, or xylose). Molar percentage of monosaccharide (MOS%) was calculated from the equation: MOS% = {[MOS] / ([Ara] + [Gal] + [Glc] + [Xyl])} × 100, where MOS indicates the monosaccharide of Ara, Gal, Glc, or Xyl.

DP was calculated by the summation of hexose (glucose and galactose) and pentose (arabinose and xylose) molar percentages, and the equation was expressed as follows: DP = (MW–18) / {(%hexose × 162/100) + (%pentose × 132/100)}, whereas MW was obtained from the above gel filtration HPLC analyses.

Accordingly, the XMS average DP 63.7 has the molar concentrations of 2.17, 2.05, 4.15, and 3.29 mM for Ara, Gal, Glc, and Xyl, respectively. Based on the above equation, MOS% of Ara = {2.17 / (2.17 + 2.05 + 4.15 + 3.29)} × 100 = 18.6%. With the same calculation, MOS% of Gal, Glc, and Xyl was obtained as 17.5, 35.8, and 28.1, respectively. The MW of XMS average DP 63.7 determined by the gel filtration HPLC was 9,445 Da and %hexose = 17.5 + 35.8 = 53.3 where %pentose = 18.6 + 28.1 = 46.7. Following the above calculation, DP = (9,445–18) / {(53.3 × 162/100) + (46.6 × 132/100)} = 63.7 (Table 2).

2.3. Curcumin solubility enhancement test. The curcumin (Nacalai) working standard was prepared by dissolving 1 mg/mL curcumin in absolute ethanol and subsequently diluting it with 10%, v/v, ethanol in water. The absorbance of the solution was determined at 440 nm by a UV–Vis spectrophotometer (U-2900, Hitachi, Japan), and the calibration curve was constructed with 0.5–10 μg/mL. Phase solubility studies were prepared as follows: an excess quantity of curcumin (1 mg) was taken into microcentrifuge tubes, and a fixed volume (100 μL) of distilled water, or water containing two concentrations of 0.5 and 1.0%, w/v, for polysaccharides including tamarind seed xyloglucan, λ-carrageenan (disulfate galactose: monosulfate galactose: galactose, 1: 2.3: 3.3, Wako Pure Chemical Industries, Osaka, Japan), amylopectin (Wako), gum arabic (rhamnose: arabinose: galactose: glucuronic acid, 1.5: 3.1: 7.9: 1, Nacalai), pectin (rhamnose: arabinose: glucose: galacturonic acid, 1: 1.4: 19.6: 18.0, Nacalai), and guar gum (mannose: galactose, 1.5: 1, Tokyo Chemical Industry Co., Ltd.). The obtained monosaccharide compositions were determined in our laboratory. The concentrations were 5 and 10%, w/v, for XOSs and XMSs. The tubes were frequently mixed by vortexing at 25 °C for 6 h. Subsequently, the supernatant was taken by centrifugation (12,000 ×*g*, 25 °C, 10 min) and carefully transferred to the incipient tubes, where the method was repeated twice. A portion of the supernatant was diluted with 10% v/v ethanol, and the curcumin concentration was determined accordingly. The solubility experiments were conducted in triplicate. The equilibrium constant (K_s) of curcumin complexed with XMS (average DP 19, 0–50%,

w/v) was determined from the phase solubility diagram according to our previous works (Lang et al., 2014).

2.4. Hydrophobic binding capacity. Curcumin is a non-fluorescent compound in aqueous media but yields a large fluorescence in a nonpolar state or some regions of low polarity. The binding affinity of curcumin and XMS was determined by the following method. A fixed volume (0.9 mL) of pure curcumin in water (0.54 μM) was mixed with an XMS average DP of 19 (0.1 mL, 0–20 mg/mL). Complex formation was monitored at an excitation wavelength of 420 nm and an emission intensity of 522.8 nm. The association constant (K_c) was determined according to previous methods (Lang et al., 2022b).

3. Results and discussion

3.1. Solubilizing ability of polysaccharides to curcumin. Some polysaccharides (e.g., α-(1→4)-glucan) exhibit remarkable hydrophobic character arising from stereochemical constraints on the chain (Sundari, Raman, & Balasubramanian, 1991). Nevertheless, Viral et al. (2010) reported that guar gum enhanced the solubility of the licofelone drug approximately 1.2-fold compared to the pure drug (9 μg/mL) by claiming the swelling nature of the carrier. The MWs of six water-soluble polysaccharides were determined by gel filtration HPLC (Fig. S2A): amylopectin (1,086 kDa), tamarind seed xyloglucan (1,075 kDa), λ-carrageenan (1,046 kDa), guar gum (980 kDa), pectin (242 and 21 kDa), and gum arabic (164 kDa). We quantified curcumin solubility with the liquid portion of six polysaccharides with the formulation of 0.5 and 1%, w/v, and the results in Fig. S2B indicate the best solubility obtained with tamarind seed xyloglucan (48.4-fold of curcumin solubilized in water, 1-fold = 0.2 μg/mL or 0.54 μM curcumin at 25 °C). This is many-fold greater than the ability of λ-carrageenan > guar gum > gum arabic > pectin > amylopectin (7.9-, 2.6-, 3.1-, 1.5- and 1-fold). D-xylose is a five-carbon sugar and has a relatively high partition coefficient to polystyrene gel by ordering: (D-xylose, D-arabinose) > D-glucose > D-galactose (Janado & Yano, 1985). In addition, the structural features of xyloglucan are a linear flexible coil conformation and chain fairly stiff (Park & Cosgrove, 2015). These reasons might be a crucial contribution to hydrophobic bonding with hydrophobic ligands because the three-dimensional shape of the cellulose backbone with a ribbon-like conformation was suggested for incapability (Sundari et al., 1991). Nevertheless, xyloglucan molecules facilely aggregate even in very dilute solutions (Kozioł, Cybulska, Pieczywek, & Zdunek, 2015) and form a viscous gel after interaction with curcumin. This polysaccharide property might limit the application of xyloglucan as a carrier. We further performed the partial depolymerization of tamarind seed xyloglucan by two hydrolysis methods, as the smaller chains are usually more soluble and less viscous than the larger ones (Guo et al., 2017).

Acid-depolymerized products from other five polysaccharides displayed the same curcumin-solubilizing ability as their parental chains.

3.2. Solubilizing activity of XMSs obtained from partial hydrolyses to curcumin. Tamarind seed xyloglucan has an average MW of 1,075 kDa with mol% values of 48.1, 32.5, 14.4, and 5.0 for glucose, xylose, galactose, and arabinose, respectively (Table 1). Varying the incubation time from 2–5 h in HCl hydrolysis resulted in three samples with a plausible yield of 30.7–53.7% (Table 1), and their average DPs of 97.1, 34.3, and 29.6 decreased consistently with the incubation time. The elution patterns obtained by gel filtration HPLC are shown in Fig. 1A, revealing a single peak. Compared with the parent xyloglucan, the sugar composition of these fragments decreased in galactose content (8.3–3.4 mol%) and was free of arabinose residues as they were acid-labile. The glucose residues became predominant (57.6–67.3 mol%) corresponding to the main chain of heat-insusceptible β-(1→4)-cellulose that is always aggregated. TV catalyzed the hydrolysis of tamarind seed xyloglucan to a mixture of shorter chains predicated on an incubation time (40 min, 1 h, and 2 h). Three samples with average DPs of 121.7, 73.1, and 28.0 have a monomer composition similar to that of the parent chain (with only a lower arabinose content) and provided better yields of 40.3–78.2% (Table 1). The results obtained from the phase solubility test for curcumin in Fig. 1B denoted that the moderate chain length (average DP 28.0) obtained from cellulase hydrolysis has a better capacity to improve the curcumin solubility to 31.9 ± 0.29-fold at 10%, w/v, than the longer average DP of 73.1 and 121.7. The longer XMS resulted in subsequent precipitation with curcumin binding.

Table 1. Properties of XMSs prepared from the partial hydrolyses of tamarind seed xyloglucan.

	Digestion Time	Average DP	Yield (%)	Monosaccharide composition (MOS%)			
				Ara	Gal	Glc	Xyl
Intact xyloglucan	-	7,128	-	5.0	14.4	48.1	32.5
HCl hydrolysis	2 h	97.1	53.7	0.0	8.3	57.6	34.1
	4 h	34.3	35.7	0.0	4.4	63.0	32.6
	5 h	29.6	30.7	0.0	3.4	67.3	29.3
Cellulase* hydrolysis	40 min	121.7	78.2	2.1	15.7	46.9	35.3
	1 h	73.1	79.5	2.6	15.5	46.8	35.1
	2 h	28.0	40.3	0.4	16.4	48.8	34.4

* is *Trichoderma viride* cellulase from Sigma (TV).

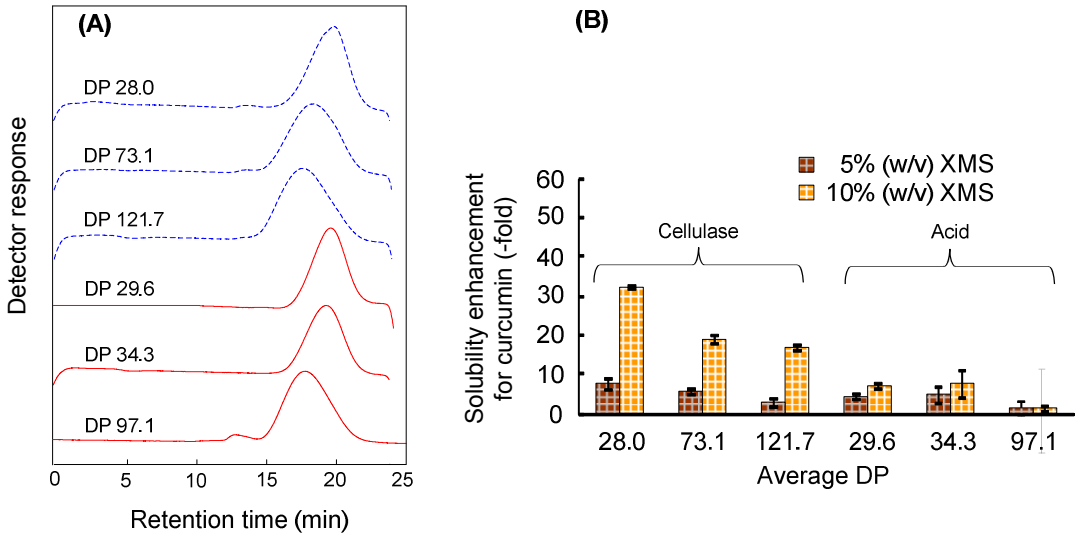

277

278 **Fig. 1.** (A) HPLC gel filtration elution profiles of tamarind seed xyloglucan hydrolysates obtained
279 from TV digestion (average DPs of 28.0, 73.1, and 121.7, dashed lines) and acid hydrolysis
280 (average DPs of 29.6, 34.3, and 97.1, dark lines). (B) Solubility enhancement of curcumin by the
281 addition of six XMSs obtained from cellulase and acid hydrolysis with 5%, w/v, and 10%, w/v,
282 compared with the solubility of curcumin in water (1-fold).

283

284 **3.3. Cleavage action of three fungal cellulases.** It is important to obtain an adequate amount of
285 active XMS samples and reproducible methods. Therefore, the action of cellulase was reconsidered,
286 and three commercial sources of fungal cellulase were compared. Their purity was visualized by
287 SDS–PAGE analysis (Fig. 2A). It reveals that all three proteins have the largest monomer with a
288 similar size of ca. 67 kDa corresponding to monomeric endoglucanase protein (Irshad et al., 2013).
289 AN obviously has additional two bands (MWs of 30 and 40 kDa), agreeing with the report of Das,
290 Bhattacharya, Roopa, & Yashoda (2011), which did not identify the cellulase activity in both
291 proteins.

292

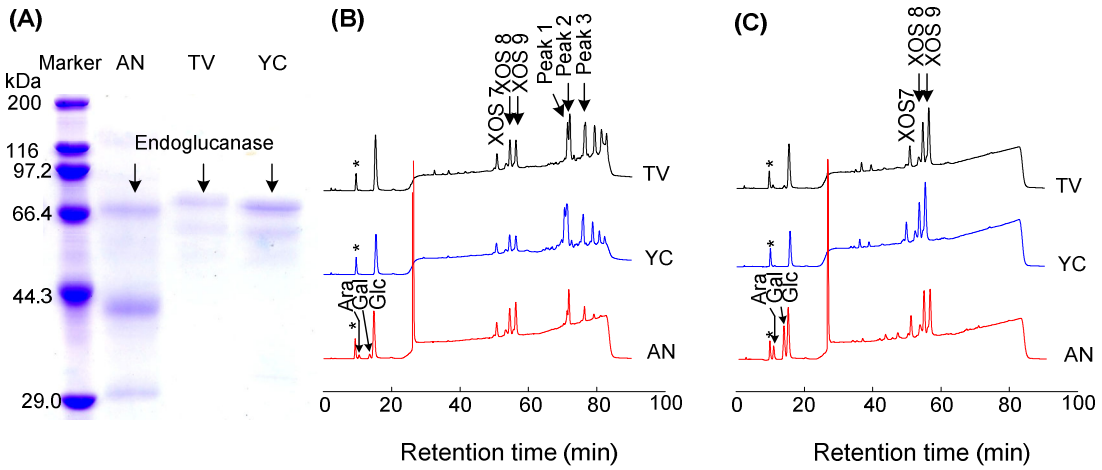

Fig. 2. (A) SDS–PAGE image comparing the commercial cellulase proteins. Lane 1, molecular mass marker; Lane 2, AN; Lane 3, TV, and Lane 4, YC. Arrows indicate endoglucanases. HPAEC-PAD analysis of the cellulase reaction mixture from TV, YC, and AN with incubation times of 2 h (B) and 24 h (C). Peaks labeled: peak 1 or XMS-A, average DP 15.8; peak 2 or XMS-B, average DP 16.6; and peak 3 or XMS-C, average DP 22.8. XOS 7, 8, and 9 are xyloglucan heptaose, octaose, and nonaose, respectively. * represents the internal standard myo-inositol.

The enzymatic products at 2 h were mainly composed of three groups of monosaccharides (at retention times of 10–16 min), oligosaccharides, XOSs 7, 8, and 9 (50–57 min), and XMSs (70–85 min), in which the last one showed a large variety of peaks (Fig. 2B). After 24 h, the sugars with DPs higher than XOS 9 were no longer present (Fig. 2C). The most commonly observed monosaccharide, in all cases, was glucose (15.94 min) and with small amounts of galactose (14.02 min) and arabinose (11.40 min) occurring in AN. This result indicated that AN has a side reaction of other hydrolytic activities, likely β-D-galactosidase and α-L-arabinosidase, removing some galactosyl and arabinose residues (Fig. 2B and 2C). Another side reaction of α-D-xylosidase was not detected. YC was more highly restricted in its specificity to endo-(1→4)-β-D-glucanase with no side-reaction and exhibited the highest contents of representative XMS-A (peak 1, 70.68 min) and XMS-B (peak 2, 71.27 min) compared with the other two cellulases (Fig. 2B and Fig. 3). The mechanism of cellulase action on xyloglucan has not been fully established. We proposed a mechanism involving the cleavage of random internal β-(1→4)-glucan at the unsubstituted parts and further access to more highly substituted regions. Highly branched regions with arabinose substitution of the main chain might be less accessible. This is evidenced by traces of insoluble residuals that remained from hydrolysis with a high ratio of arabinose (16.7 mol%) indicated in Table 2 according to the next session. We propose an alternative way to utilize fungal cellulase for the removal of arabinose-substituted regions in the case of high-viscosity samples.

Table 2. Properties of XMSs fractionated from the enzyme[a] hydrolysis of tamarind seed xyloglucan[b].

Methanol Precipitation (%)	Amount (g)	Yield (%)	DP	Monosaccharide composition (MOS%)			
				Ara	Gal	Glc	Xyl
Insoluble part	0.31	2.1	N.D.	16.7	12.6	35.0	35.7
≤ 60	2.51	16.7	63.7	18.6	17.5	35.8	28.1
60–70	2.31	15.4	24.3	0.3	17.8	51.1	30.8
80–95	1.91	12.7	15.4	0.5	17.5	48.7	33.3
> 95	1.20	8.0	9.0	-	16.4	47.8	35.9
XMS-A	N.D.	N.D.	15.8 (16.2[c])	-	12.6	50.1	37.0
XMS-B	N.D.	N.D.	16.6 (17.2[c])	-	17.0	48.2	34.5

[a] is *Trichoderma viride* cellulase from Seshin Pharmaceutical (YC).

[b] = 15 g.

[c] is DP calculated using mass spectrometry data (MWs of XMS-A and XMS-B: 2,454.78 and 2,616.82, respectively).

N.D. = not determined.

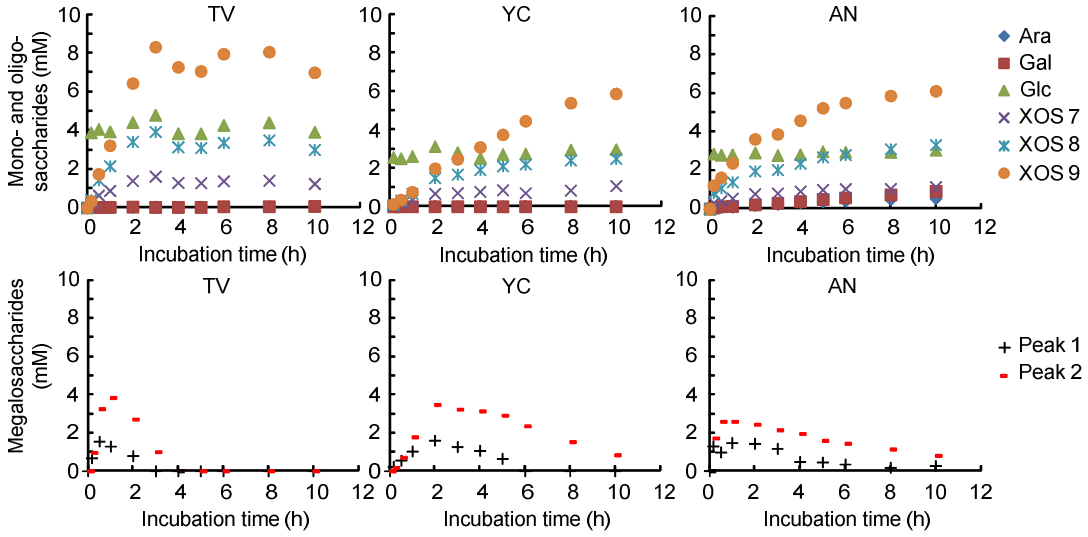

Fig. 3. Time course production of monosaccharides, XOSs, and XMSs from tamarind seed xyloglucan by cellulase digestion. The cellulases utilized were the commercially available TV, YC, and AN.

3.4. Isolation of active XMSs. Four fragments from YC hydrolysates were obtained by sequential methanol precipitation, and the chromatograms are presented in Fig. 4A. The largest fragment with an average DP of 63.7 was taken by ≤ 60%, v/v, methanol. The arabinose content appeared to be

the average highest (Table 2). Only these samples showed high viscosity after being dissolved in water. A fragment of 60–70%, v/v, methanol with an average DP of 24.3 showed the main composition with XMS-C (peak 3 denoted in Fig. 2B, 75.8 min) combined with a mixture of slightly shorter and larger sizes. A fragment of 80–95%, v/v, with an average DP of 15.4 shows mainly pure XMS-A and XMS-B. A short fragment from > 95%, v/v, methanol contained only XOSs with an average DP of 9.0. Fig. 4B presents the results of phase solubility enhancement tests for curcumin, which were almost similar between XMSs with average DPs of 24.3 (36.1 ± 6.87-fold) and 15.4 (36.6 ± 3.63-fold) but twice as large as XOSs (17.0 ± 3.84-fold) at 10%, w/v. Next, the samples were purified by preparative HPLC. The purity of these fractions of XOS 7–9, XMS-A, and XMS-B appeared in HPAEC-PAD chromatograms (Fig. 5A). XMS-A fraction displays two peaks (peak 1 and peak 1′), and the saccharide of peak 1′ is different from XMS-B of peak 2 since molecular masses of XMS-A and XMS-B are distinct (Fig. 5B). ESI mass spectrometry allowed the MW determination of the purified XMS-A and XMS-B and ascertained their DPs as follows. Fragment $[M + 2H]^{2+}$ or $[M + 2Na]^{2+}$ ions of 1,238.89 and 1,319.91 were observed for XMS-A and XMS-B, respectively (Fig. 5B), corresponding to MWs of 2,454.78 and 2,616.82. These results agree with the average MWs of 2,391 and 2,529 obtained by gel chromatography in our analysis. Calculations based on the sugar content in Table 2 present new average DP values of 16.2 and 17.2 for XMS-A and XMS-B, respectively. The results of the structure analysis of XMS-B by cellulase hydrolysis showed that the composition led to further hydrolysis to an equimolar mixture of XOS 8 and 9. This structure could be characterized by the presence of a β-(1→4)-glycosidic linkage in the chain, and in conclusion, XMS-B was a branched $Gal_3Glc_8Xyl_6$. The curcumin solubility was 24.1 ± 0.4-fold for XMS-A and 40.9 ± 0.7-fold for XMS-B. Purified XOS 9 was 18.9 ± 0.64-fold, and its capacity was better than those of shorter sized XOS 8 and XOS 7. This observation suggested that xyloglucan with a longer chain length was more effective in dissolving curcumin, as it contained a larger amount of xylosyl substitution for a better conformation, promoting hydrophobic interactions, and galactosyl substituents assisted in water solubility. In addition, the ideal chain should not appear to be influenced by the high viscosity arising from arabinose.

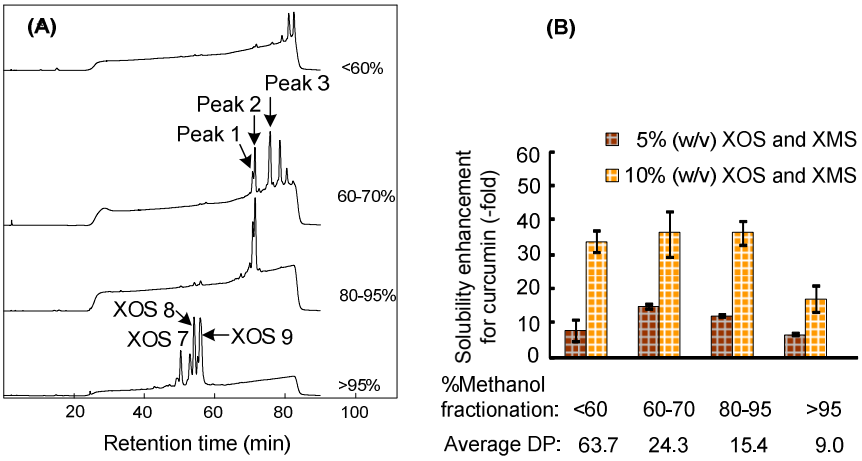

Fig. 4. (A) HPAEC-PAD elution profiles of YC-digested XMSs obtained from fractionation by methanol. (B) The solubility enhancement of curcumin with the addition of XOS and XMS at 5 and 10%, w/v, compared with the solubility of curcumin in water (1-fold).

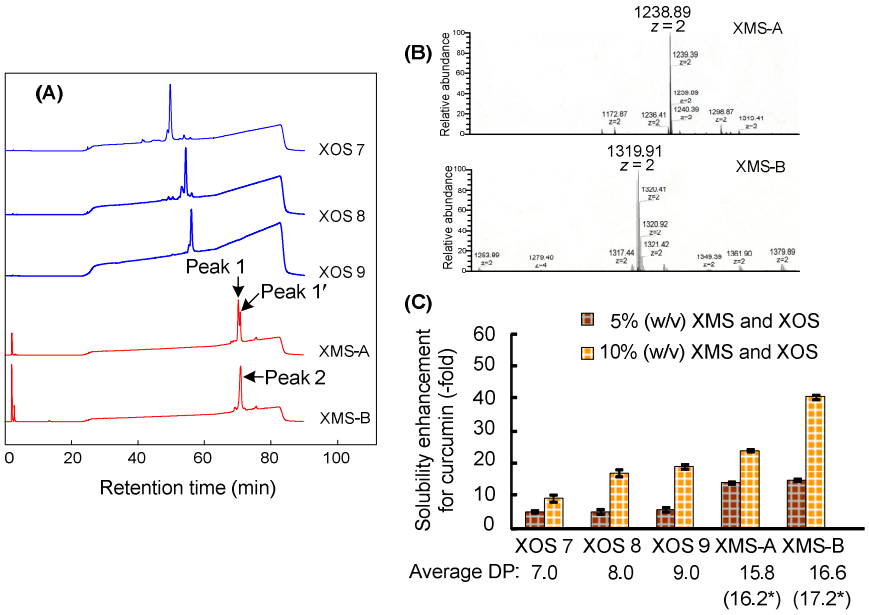

Fig. 5. (A) HPAEC-PAD elution profiles of purified tamarind seed xyloglucan hydrolysates by preparative HPLC. (B) Electrospray ionization mass spectrometry analysis of purified XMS-A and XMS-B separated by HPLC. (C) The solubility enhancement of the corresponding samples. * is new DPs calculated using mass spectrometry data.

3.5. Solubilizing ability of XMS average DP 19 to curcumin. Based on the results of Fig. 5C, XMS-B yielded the best curcumin solubilization, implying that XMS-B-rich fraction is suitable for practical preparation of functional MS. The XMS fraction with 60–75%, v/v, methanol was considered to improve more XMS-B than 60–70%, v/v, methanol fraction (Fig. 4). As expected,

the sample (XMS average DP 19; 20% yield) contained more XMS-B (Fig. 6A). The product was highly soluble in water at room temperature. We achieved a solubility enhancement of ca. 25.3 ± 0.4-fold that of curcumin at 10%, w/v, XMS, which was lower than expected probably due to some contaminants of XOSs (Fig. 6B). To discard XOSs, the dialysis using a membrane with a MW cutoff of 2 kD against water is recommendable for removal of saccharides having an average DP less than 12 (Lang et al., 2022b). Nevertheless, the higher solubility enhancement was more accessible at higher XMS concentrations, as evidenced by the phase solubility diagram (Fig. 6B). The increase in nonlinear type as a function of XMS concentrations corresponded to the A_P-type profile. This can be implied by the fact that the complex is first-order concerning curcumin but second- or higher-order concerning XMS concentration. The maximum solubility of curcumin was achieved at 97 μM or more than a 180-fold increase over curcumin solubility in water with 50%, w/v, XMS average DP 19, and the yellow color could be visually perceived as transparent (Fig. 6C). Fluorescence spectra were recorded for curcumin solutions in increasing concentrations of XMS average DP 19 (1–20 mg/mL or equivalent to 0.34–6.9 mM). Curcumin in water excited at 420 nm was weakly fluorescent and had a broad spectrum centered at approximately 530 nm. During the titrations, curcumins exhibited a blueshift of the spectral band to shorter wavelengths (Fig. 7A). This phenomenon mainly indicated the movement of curcumin from a polar to a less polar environment. This observation is in good accordance with the binding of curcumin and β-lactoglobulin protein, which hydrophobic interactions contribute (Sneharani, Karakkat, Singh, & Rao, 2010). Fig. 7B shows the double reciprocal plots of the results obtained by integrating the XMS dropwise. The binding constant was estimated to be 68 M^{-1}.

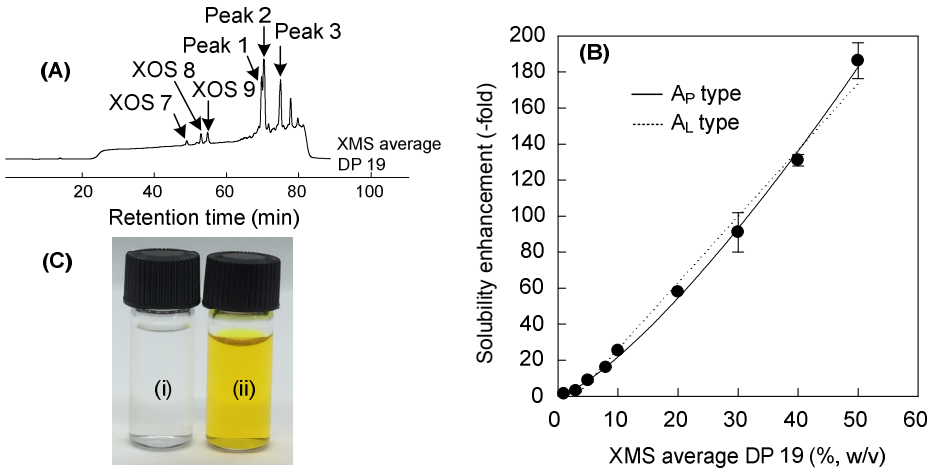

Fig. 6. (A) HPAEC-PAD chromatogram of XMS average DP 19 fractionated by 60–75%, v/v, methanol. (B) Phase solubility diagram of curcumin with the addition of XMS. Average DP 19 from 0–50%, w/v. (C) Curcumin solubilized in (i) water and (ii) 50%, w/v, XMS average DP 19.

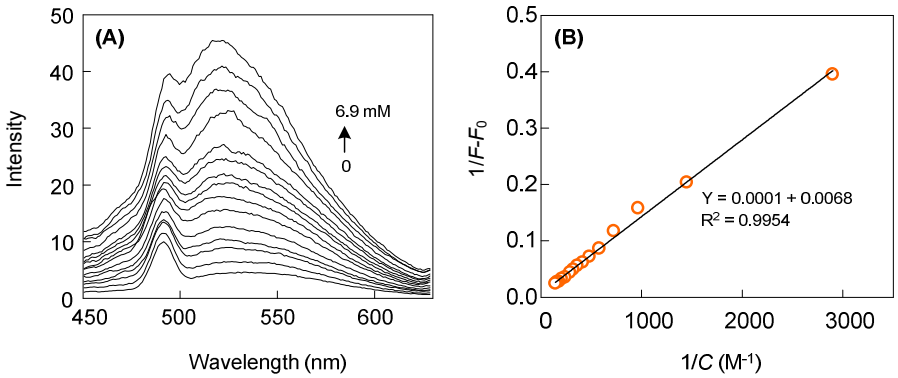

Fig. 7. (A) Fluorescence spectra of curcumin with increasing concentrations of XMS average DP 19 in the direction of the arrow from 0–20 mg/mL (equivalent to 0–6.9 mM). (B) Benesi-Hildebrand double reciprocal plot of the emission intensity at 522.8 nm against the series of XMS concentrations where the I_0 value was 4.

Xyloglucan enhanced curcumin solubility by 48.4-fold at its low concentration of 1%, w/v. Its hydrophobic coil-structure contributes to curcumin-solubilizing ability. However, the concentration is difficult to increase more because of being highly viscous and forming insoluble curcumin-xyloglucan complex. XMS average DP 19 increased the curcumin solubility by 25- or 180-fold at its 10 or 50% (w/v) concentration, respectively. XMS with molecular mass ≤ 10 kDa does not form coil structure (Hayashi, 1989; Tabuchi, Mori, Kamisaka, & Hoson, 2001). We have no reasonable explanation about curcumin-solubilizing mechanism mediated by XMS. The longer size or monosaccharides (arabinose, galactose, xylose) of XMS might contribute to hydrophobicity and interact with curcumin. Formed curcumin-XMS complex becomes water-soluble due to high aqueous solution of XMS.

4. Conclusion

The aqueous solubility of curcumin was improved remarkably by tamarind seed xyloglucan solution compared with those of the five polysaccharides. The appropriate size preparation strategy could be established in this study, not only in accordance with the polysaccharide shortening method (Guo, Hu, Wang, & Ai, 2017), but our methods also selectively maintained (e.g., xylose) or removed (e.g., arabinose) the fine composition of tamarind seed xyloglucan. The partial depolymerization by YC cellulase at 2 h of incubation enabled the reproducible preparation of functional XMS. The active sizes with average DPs of 15.4–24.3 showed a similar capacity for curcumin solubility to ca. 36–40-fold, and hence, the XMS isolation with 60–75% methanol precipitation was approached. The longer DPs caused the precipitation of gel complexes and subsequently minimized curcumin solubility in the aqueous phase. The typical MS with average DP 19 was readily dissolved in water at room temperature, and the higher the

XMS concentration was, the higher the amount of dissolved curcumin. The daily dose of curcumin was determined accordingly. The XMS functionality and textural property thus fit well in prevalence common household requisites. The health science formulation development will be further clarified in the following work.

Figure captions

Fig. 1. (A) HPLC gel filtration elution profiles of tamarind seed xyloglucan hydrolysates obtained from TV digestion (average DPs of 28.0, 73.1, and 121.7, dashed lines) and acid hydrolysis (average DPs of 29.6, 34.3, and 97.1, dark lines). (B) Solubility enhancement of curcumin by the addition of six XMSs obtained from cellulase and acid hydrolysis with 5%, w/v, and 10%, w/v, compared with the solubility of curcumin in water (1-fold).

Fig. 2. (A) SDS–PAGE image comparing the commercial cellulase proteins. Lane 1, molecular mass marker; Lane 2, AN; Lane 3, TV, and Lane 4, YC. Arrows indicate endoglucanases. HPAEC-PAD analysis of the cellulase reaction mixture from TV, YC and AN with incubation times of 2 h (B) and 24 h (C). Peaks labeled: peak 1 or XMS-A, average DP 15.8; peak 2 or XMS-B, average DP 16.6; and peak 3 or XMS-C, average DP 22.8. XOS 7, 8 and 9 are xyloglucan heptaose, octaose, and nonaose, respectively. * represents the internal standard myo-inositol.

Fig. 3. Time course production of monosaccharides, XOSs, and XMSs from tamarind seed xyloglucan by cellulase digestion. The cellulases utilized were the commercially available TV, YC, and AN.

Fig. 4. (A) HPAEC-PAD elution profiles of YC-digested XMSs obtained from fractionation by methanol. (B) The solubility enhancement of curcumin with the addition of XOS and XMS at 5 and 10%, w/v, compared with the solubility of curcumin in water (1-fold).

Fig. 5. (A) HPAEC-PAD elution profiles of purified tamarind seed xyloglucan hydrolysates by preparative HPLC. (B) Electrospray ionization mass spectrometry analysis of purified XMS-A and XMS-B separated by HPLC. (C) The solubility enhancement of the corresponding samples. * is new DPs calculated using mass spectrometry data.

Fig. 6. (A) HPAEC-PAD chromatogram of XMS average DP 19 fractionated by 60–75%, v/v, methanol. (B) Phase solubility diagram of curcumin with the addition of XMS. Average DP 19 from 0–50%, w/v. (C) Curcumin solubilized in (i) water and (ii) 50%, w/v, XMS average DP 19.

Fig. 7. (A) Fluorescence spectra of curcumin with increasing concentrations of XMS average DP 19 in the direction of the arrow from 0–20 mg/mL (equivalent to 0–6.9 mM). (B) Benesi-Hildebrand double reciprocal plot of the emission intensity at 522.8 nm against the series of XMS concentrations where the I_0 value was 4.

Acknowledgments

This study was supported partially by a Program for Promotion of Basic and Applied Research for Innovations in Biooriented Industry (BRAIN), Japan [Grant numbers 25001A, 26062B] and the Japan Society for the Promotion of Science KAKENHI [Grant numbers 17H03801, 19KK0147]. The manuscript received English proofreads from Elsevier's Author Services.

CRediT authorship contribution statement

Weeranuch Lang: Conceptualization, Investigation, Formal analysis, Writing - original draft - review & editing. Takayoshi Tagami: Resources, Supervision. Hye-Jin Kang: Formal analysis, Investigation. Masayuki Okuyama: Data curation, Resources. Nobuo Sakairi: Conceptualization, Supervision. Atsuo Kimura: Writing - review & editing. Resources, Supervision, Funding acquisition, Project administration.

Declaration of Competing Interest. The authors report no declarations of interest.

References

Bengtsson, S., Andersson, R., Westerlund, E., & Åman, P. (1992). Content, structure and viscosity of soluble arabinoxylans in rye grain from several countries. *Journal of the Science of Food and Agriculture*, *58*(3), 331–337. https://doi.org/10.1002/jsfa.2740580307

Das, A., Bhattacharya, S., Roopa, K. S., & Yashoda, S. S. (2011). Microbial utilization of agronomic wastes for cellulase production by *Aspergillus niger* and *Trichoderma viride* using solid-state fermentation. *Dynamic Biochemistry, Process Biotechnology and Molecular Biology*, *5*(2), 18–22

Guo, M. Q., Hu, X., Wang, C., & Ai, L. (2017). Polysaccharides: structure and solubility. In *Solubility of Polysaccharides* (Issue April). https://doi.org/10.5772/intechopen.71570.

Hayashi, T. (1989). Xyloglucans in the primary cell wall. *Annual Review of Plant Physiology and Plant Molecular Biology*, 40, 139–168. https://doi.org/10.1146/annurev.pp.40.060189.001035

Irshad, M., Anwar, Z., But, H. I., Afroz, A., Ikram, N., & Rashid, U. (2013). The industrial applicability of purified cellulase complex indigenously produced by *Trichoderma viride* through solid-state bio-processing of agro-industrial and municipal paper wastes. *BioResources*, *8*(1), 145–157. https://doi.org/10.15376/biores.8.1.145-157

Janado, M., & Yano, Y. (1985). Hydrophobic nature of sugars as evidenced by their differential affinity for polystyrene gel in aqueous media. *Journal of Solution Chemistry*, *14*(12), 891–902. https://doi.org/10.1007/BF00646298

Kozioł, A., Cybulska, J., Pieczywek, P. M., & Zdunek, A. (2015). Evaluation of structure and assembly of xyloglucan from tamarind seed (*Tamarindus indica* L.) with atomic force

507 microscopy. *Food Biophysics*, *10*(4), 396–402. https://doi.org/10.1007/s11483-015-9395-2
508 Lang, W., Kumagai, Y., Sadahiro, J., Maneesan, J., Okuyama, M., Mori, H., Sakairi, N., & Kimura,
509 A. (2014). Different molecular complexity of linear-isomaltomegalosaccharides and β-
510 cyclodextrin on enhancing solubility of azo dye ethyl red: Towards dye biodegradation.
511 *Bioresource Technology*, *169*, 518–524. https://doi.org/10.1016/j.biortech.2014.07.025
512 Lang, W., Kumagai, Y., Sadahiro, J., Saburi, W., Sarnthima, R., Tagami, T., Okuyama, M., Mori,
513 H., Sakairi, N., Kim, D., & Kimura, A. (2022a). A practical approach to producing
514 isomaltomegalosaccharide using dextran dextrinase from *Gluconobater oxydans* ATCC
515 11894. *Applied Microbiology and Biotechnology*, *106*, 689–698.
516 https://doi.org/10.1007/s00253-021-11753-6
517 Lang, W., Kumagai, Y., Habu, S., Sadahiro, J., Tagami, T., Okuyama, M., Kitamura, S., Sakairi, N.,
518 & Kimura, A. (2022b). Physicochemical functionality of chimeric isomaltomegalosaccharides
519 with α-(1 → 4)-glucosidic segments of various lengths. *Carbohydrate Polymers*, *291*(April),
520 119562. https://doi.org/10.1016/j.carbpol.2022.119562
521 Mahajan, H. S., Tyagi, V., Lohiya, G., & Nerkar, P. (2012). Thermally reversible xyloglucan gels
522 as vehicles for nasal drug delivery. *Drug Delivery*, *19*(5), 270–276.
523 https://doi.org/10.3109/10717544.2012.704095
524 Majee, S. B., Avlani, D., & Biswas, G. R. (2016). Non-starch plant polysaccharides:
525 Physicochemical modifications and pharmaceutical applications. *Journal of Applied*
526 *Pharmaceutical Science*, *6*(10), 231–241. https://doi.org/10.7324/JAPS.2016.601033
527 Mangolim, C. S., Moriwaki, C., Nogueira, A. C., Sato, F., Baesso, M. L., Neto, A. M., & Matioli,
528 G. (2014). Curcumin-β-cyclodextrin inclusion complex: Stability, solubility, characterisation
529 by FT-IR, FT-Raman, X-ray diffraction and photoacoustic spectroscopy, and food application.
530 *Food Chemistry*, *153*, 361–370. https://doi.org/10.1016/j.foodchem.2013.12.067
531 Nguyen, T. T. H., Si, J., Kang, C., Chung, B., Chung, D., & Kim, D. (2017). Facile preparation of
532 water soluble curcuminoids extracted from turmeric (*Curcuma longa* L.) powder by using
533 steviol glucosides. *Food Chemistry*, *214*, 366–373.
534 https://doi.org/10.1016/j.foodchem.2016.07.102
535 Niemann, C., Carpita, N. C., & Whistler, R. L. (1997). Arabinose-containing oligosaccharides from
536 tamarind xyloglucan. *Starch/Staerke*, *49*(4), 154–159.
537 https://doi.org/10.1002/star.19970490407
538 Park, Y. B., & Cosgrove, D. J. (2015). Xyloglucan and its interactions with other components of
539 the growing cell wall. *Plant and Cell Physiology*, *56*(2), 180–194.
540 https://doi.org/10.1093/pcp/pcu204
541 Prasad, S., Tyagi, A. K., & Aggarwal, B. B. (2014). Recent developments in delivery,
542 bioavailability, absorption and metabolism of curcumin: The golden pigment from golden

spice. *Cancer Research and Treatment*, *46*(1), 2–18. https://doi.org/10.4143/crt.2014.46.1.2

Sapkal, S., Narkhede, M., Babhulkar, M., Mehetre, G., & Rathi, A. (2013). Natural polymers: Best carriers for improving bioavailability of poorly water soluble drugs in solid dispersions. *Marmara Pharmaceutical Journal*, *17*(2), 65–72. https://doi.org/10.12991/201317375

Satoh, S., Tateishi, A., & Sugiyama, S. (2013). Preparation of a xyloglucan oligosaccharide mixture from tamarind seed gum and its promotive action on flower opening in carnation cultivars. *Journal of the Japanese Society for Horticultural Science*, *82*(3), 270–276. https://doi.org/10.2503/jjshs1.82.270

Sharma, A., Hawthorne, S., Jha, S. K., Jha, N. K., Kumar, D., Girgis, S., Goswami, V. K., Gupta, G., Singh, S., Dureja, H., Chellappan, D. K., & Dua, K. (2021). Effects of curcumin-loaded poly(lactic-co-glycolic acid) nanoparticles in MDA-MB231 human breast cancer cells. *Nanomedicine*, *16*(20), 1763–1773. https://doi.org/10.2217/nnm-2021-0066

Sneharani, A. H., Karakkat, J. V., Singh, S. A., & Rao, A. G. A. (2010). Interaction of curcumin with ß-lactoglobulin;stability, spectroscopic analysis, and molecular modeling of the complex. *Journal of Agricultural and Food Chemistry*, *58*(20), 11130–11139. https://doi.org/10.1021/jf102826q

Sone, Y., & Sato, K. (1994). Measurement of oligosaccharides derived from tamarind xyloglucan by competitive elisa assay. *Bioscience, Biotechnology, and Biochemistry*, *58*(12), 2295–2296. https://doi.org/10.1271/bbb.58.2295

Sundari, C. S., Raman, B., & Balasubramanian, D. (1991). Hydrophobic surfaces in oligosaccharides: linear dextrins are amphiphilic chains. *Biochimica et Biophysica Acta*, *1065*, 35–41. https://doi.org/doi: 10.1016/0005-2736(91)90007-u

Tabuchi, A., Mori, H., Kamisaka, S., & Hoson, T. (2001). A new type of endo-xyloglucan transferase devoted to xyloglucan hydrolysis in the cell wall of azuki bean epicotyls. *Plant and Cell Physiology*, *42*(2), 154–161. https://doi.org/10.1093/pcp/pce016

Thoma, J. A., Wright, H. B., & French, D. (1959). Partition chromatography of homologous saccharides on cellulose columns. *Archives of Biochemistry and Biophysics*, *85*(2), 452–460. https://doi.org/10.1016/0003-9861(59)90510-7

Victorelli, F. D., Salvati Manni, L., Biffi, S., Bortot, B., Buzzá, H. H., Lutz-Bueno, V., Handschin, S., Calixto, G., Murgia, S., Chorilli, M., & Mezzenga, R. (2022). Potential of curcumin-loaded cubosomes for topical treatment of cervical cancer. *Journal of Colloid and Interface Science*, *620*, 419–430. https://doi.org/10.1016/j.jcis.2022.04.031

Viral, S., Dhiren, P., Mane, S., & Umesh, U. (2010). Solubility and dissolution rate enhancement of licofelone by using modified guar gum. *International Journal of PharmTech Research*, *2*(3), 1847–1854

Walker, J. A., Pattathil, S., Bergeman, L. F., Beebe, E. T., Deng, K., Mirzai, M., Northen, T. R.,

Hahn, M. G., & Fox, B. G. (2017). Determination of glycoside hydrolase specificities during hydrolysis of plant cell walls using glycome profiling. *Biotechnology for Biofuels*, *10*(1), 1–19. https://doi.org/10.1186/s13068-017-0703-6

Wu, Y., Mou, B., Song, S., Tan, C. P., Lai, O. M., Shen, C., & Cheong, L. Z. (2020). Curcumin-loaded liposomes prepared from bovine milk and krill phospholipids: Effects of chemical composition on storage stability, in-vitro digestibility and anti-hyperglycemic properties. *Food Research International*, *136*(May), 109301. https://doi.org/10.1016/j.foodres.2020.109301

Yadav, S., Singh, A. K., Agrahari, A. K., Sharma, K., Singh, A. S., Gupta, M. K., Tiwari, V. K., & Prakash, P. (2020). Making of water soluble curcumin to potentiate conventional antimicrobials by inducing apoptosis-like phenomena among drug-resistant bacteria. *Scientific Reports*, *10*(1), 1–22. https://doi.org/10.1038/s41598-020-70921-2

Zhang, X., Lu, Y., Zhao, R., Wang, C., Wang, C., & Zhang, T. (2022). Study on simultaneous binding of resveratrol and curcumin to β-lactoglobulin: Multi-spectroscopic, molecular docking and molecular dynamics simulation approaches. *Food Hydrocolloids*, *124*, 107331. https://doi.org/https://doi.org/10.1016/j.foodhyd.2021.107331